The impact of tellurite glass on contact resistance of the fire through dielectric (FTD) c-Si solar cell with lightly doped emitter

Keming Ren, Veysel Unsur, Ahrar Chowdhury, Yong Zhang and Abasifreke Ebong

Energy Production and Infrastructure Center, Department of Electrical and Computer Engineering,
University of North Carolina at Charlotte, Charlotte, NC, 28223, USA

Abstract — In this paper, the influence of Te-glass frit on silver screen-printed contact formation in crystalline Si solar cell is reported. During fire through dielectric (FTD) contact process, the Te-glass frit enhances the formation of Ag_2Te and $PbTe$ in the reformed glass underlying the front Ag gridline. The presence of Ag_2Te, which is a semi-metal, heightens the electron tunneling probability and in turn reduces the contact resistivity. The formation of the Ag_2Te and $PbTe$ is supported by Raman spectra peaks at 79 cm^{-1}, 119 cm^{-1}, 145 cm^{-1}, 183 cm^{-1}, 195 cm^{-1} and 660 cm^{-1} for the Ag pastes after HNO_3 treatment. SEM also reveals that most metal crystallites are embedded in the glass layer rather than silicon. This means that, these glass layers play important role in the electron tunneling from Si into the Ag gridline.

Index Terms — solar energy, photovoltaic cells, contact resistance, silicon, silver telluride.

I. INTRODUCTION

Screen-printing technology is the most cost-effective method to manufacture commercial silicon solar cell. This technology involves the dispensing of Ag gridlines onto the antireflective dielectric layer on an emitter and then fire through the dielectric (FTD) to contact the underlying silicon. During the contact firing, the glass frit in the Ag paste melts, react with the dielectric through redox reaction. Then Ag ions dissolve into the molten glass in the thick film and then etch the dielectric layer. At the same time, Si dissolve into the mix. Upon cooling Ag crystallites or colloids precipitate in Si and demarcated by thin glass beneath the metal contact. Paramount in the process is to produce a contact with low series resistance that will not negatively impact the fill factor (FF).

Lightly doped emitter is needed for high efficiency solar cells because of its low surface recombination. However, the low surface concentration poses a high contact resistance potential. Theoretically, under low doping condition ($N_D < \sim 10^{17} cm^{-3}$), a Schottky barrier is formed and the electron transfers through thermionic emission[1]. When the doping concentration is in the range of $\sim 10^{17} cm^{-3} < N_D < \sim 10^{18} cm^{-3}$, thermionic-field transport is prominent which is the typical mechanism in FTD. And when $N_D > \sim 10^{18} cm^{-3}$, field emission is achieved where electrons can freely travel through the barrier with low contact resistivity. According to Yu [2], contact resistivity is proportional to the inverse square root of the emitter peak surface doping concentration. This implies, the homogeneous high sheet resistance or lightly doped emitter would require an intermediary conductor in the reformed glass (after firing) at the interface of Si/Ag to induce field emission current transport through the contact. This is done through paste modifications with appropriate additives that could lead to higher conductivity of both the contact and gridlines. In this study, the impact of such additive to PbO based Ag paste on contact resistance is studied through (i) Raman Spectrometer, (ii) SEM, and (iii) EDX analyses.

II. CURRENT TRANSPORT IN SCREEN-PRINTED CONTACTS

The three plausible current transport mechanism in screen-printed contacts include: (i) direct contact of Ag-gridline to Si. (ii) conduction by Ag crystallites through thin glass at the Si/Ag gridlines, and (iii) tunneling assisted by nano-Ag colloids, which might be highly conductive.

Cabrera et al.[3] suggested in their study that, the major current flow into the Ag gridline is through the Ag crystallites, which directly contacts with bulk Ag and the contact resistivity is less than 1 mΩ·cm^2. When the glass layer is formed right on top of Si, the contact resistivity is high, ~ 100 mΩ·cm^2. And without the Ag crystallites in Si, the contact is poor with contact resistivity of >1300 mΩ·cm^2. Kontermann et al. [4], measured the specific contact resistivity between a Ag crystallite and Si substrate as ~ 0.047 mΩ·cm^2 , which was small enough to exclude other current transport mechanisms. This stresses the necessity of the Ag crystallites for current transport from Si to Ag gridline, which is supported by theoretical calculation of the macroscopic contact resistance [5].

However, Kumar et al [6] studied Al doped Ag paste and found high efficient n-type solar cell was achieved without silver crystals where contact resistivity was 4 mΩ·cm^2. Li et al.[7], also found that there was no Ag crystallites on the emitter of the best-performing cell. This led to the conclusion that Ag crystallite are not necessary for efficient current collection. However, their study considered tunneling assisted conduction by nano-silver colloids. Thus, the electrons are transported through thick glass region by multi-step tunneling. The number of Ag colloids was critical for the conductivity of the glass layers. It was found that the higher the Ag colloids density in the glass (197 colloids/um^2), the lower the contact resistivity (5 mΩ·cm^2). However, tunneling may not be the only explanation because the thickness of the interface glass layer is >10 nm, whereas tunneling process only happens within a few nanometers. In this case, the glass should be assumed to be a conductor [8].

The current mechanism proposed were based on the study of the reaction of the Ag-paste with SiNx ARC and Si. In each of these cases, the top phosphorus surface concentration was not taken into account. Since the metal fires through the dielectric, forming contact to lightly-doped emitter with low contact

resistance it is necessary to understand how the constituents of the Ag paste impact the contact and hence the current conduction mechanism. Several studies have been carried out to understand the properties of the Ag paste, such as silver particle size [9], glass frits [10] and sintering condition [11], which can achieve not only lower contact resistance, but also lower gridline resistance. But achieving series resistance of < 0.2 Ω-cm^2 and fill factor (FF) of >82% for FTD solar cell is still a challenge. The modification of Ag paste with additives has been investigated and recently TeO_2 in conjunction with PbO. In this work, the impact of TeO_2 as an additive to the conventional PbO glass frit is reported.

III. CELL FABRICATION

Czocralski (Cz), p-type silicon wafers of ~2.5 Ω-cm resistivity were textured, diffused with phosphorus at 890° C to form emitter with 95 Ω/square. The wafers were subjected to edge isolation before the phosphorus glass removal followed by PECVD SiNx deposition with thickness of 73 nm. The wafers were then divided into four groups – for four blends of TeO_2 based glasses. For the blends, four variations based on glass transition temperature T_G, thus sixteen pastes altogether were formulated. However, only four pastes, A, B, C and D were tested in this study. Ten cells with the three bus-bar front gridlines cell structure was printed for each paste, dried before the back-Al printing plus dry. The contacts were co-fired in the state-of-the-art rapid thermal processing (RTP) infrared belt furnace at 230 inches per minute (IPM) at 815° C peak temperature. This was followed by light IV characterization.

After the IV measurements, one cell from each group was cut to measure the contact resistance. To measure the contact resistance for each paste, one cell from each group was cut into 2-mm strip. TABLE I shows the electrical parameters for the four of the pastes (A, B. C. and D) that are used in this study.

To assess the micro and nano structures the contacts associated with the four pastes, three sets of cut samples were generated for each paste; namely: (i) as fired (AF), (iii) NHO$_3$ treated to remove the silver gridline but glass left intact (HNO$_3$), and (iii) HF treated to remove the glass (HF). These samples were used to evaluate the microstructure and elemental composition in conjunction with SEM and EDX (JEOL w/ EDAX, Model 6460LV), and Raman spectrometer (HORIBA, XploRa^{TM}PLUS) excited at 532 nm.

IV. RESULT AND DISCUSSION

A. I-V characterization

TABLE I shows the electrical output parameters for the four paste samples. Paste D exhibited the highest open-circuit voltage (V_{oc}), FF (~79%), efficiency (20.03%) and lowest contact (R_c) and series (R_s) resistivities. While paste A showed the highest R_c and R_s, lowest short-circuit current (J_{sc}), V_{oc} and FF of only 46.53 %, hence the lowest efficiency of 11.42%. However, the highest efficiency of 20.05% was exhibited by cell made with paste B because of 0.2 mA/cm2 difference in Jsc. Voc for cells made with paste B and D differ only by 0.3 mV, but slightly higher contact resistance. Thus the three pastes B, C and D are quite comparable.

B. Raman Spectra

The Raman Spectrometer is used to investigate the peaks of compounds formed in the contact after firing. However, the most conclusive ones are those after HNO$_3$ etch, where the Ag gridline is etch off but the glass is intact. Fig. 1(a) shows the Raman spectra for the four pastes after HNO$_3$ etching. Pastes B, C and D show similar peaks at 79 cm^{-1}, 119 cm^{-1}, 145 cm^{-1}, 183 cm^{-1}, 195 cm^{-1} and 660 cm^{-1}. According to Qin et al.[12], the peak at 76 cm^{-1}[13], 119 cm^{-1} and 145 cm^{-1} come from Ag$_2$Te. The peak around 365 cm^{-1} and 660 cm^{-1} are due to bending vibration of TeO_2. The peaks at 119 cm^{-1}, 183 cm^{-1} and 366 cm^{-1} result from PbTe [14]. From Fig. 1(a), paste A lacks the presence of these peaks and hence Ag$_2$Te and PbTe.

To ensure where the Ag$_2$Te and PbTe are located as alluded in Fig. 1a, the HF treated samples were exposed to Raman Spectrometer. After HF treatment, which removes the glass from the contact, as seen in Fig 1(b), the peaks were hardly found. The peak at 230cm^{-1}, 303cm^{-1} and 620cm^{-1} come from Si. This is similar to the peaks exhibited by the gridline after firing. This suggests that Ag$_2$Te and PbTe are in the glass layer underlying the gridlines, which is responsible for increased conductivity of the glass layer and enhance carrier conduction into the gridlines. This supports the tunneling-assisted conduction by nano-Ag colloids. This revelation seems remarkable with a possibility of contacting emitters with low surface concentration since the contact resistance is very likely to be independent of the inverse of the peak surface concentration.

TABLE I
FOUR DIFFERENT SILVER PASTES WITH DIFFERENT TELLURITE GLASS RATIOS

Ag Paste	Voc (mV)	Jsc (mA/cm^2)	FF (%)	Efficiency (%)	Rc (Ω-cm^2)	Rs (Ω-cm^2)
A	634.3	38.68	46.53	11.42	0.83	11.6628
B	641.7	39.58	78.96	20.05	0.44	0.7274
C	641.8	39.50	78.34	19.85	0.39	0.8306
D	642.0	39.38	79.26	20.03	0.31	0.6646

(a)

(b)
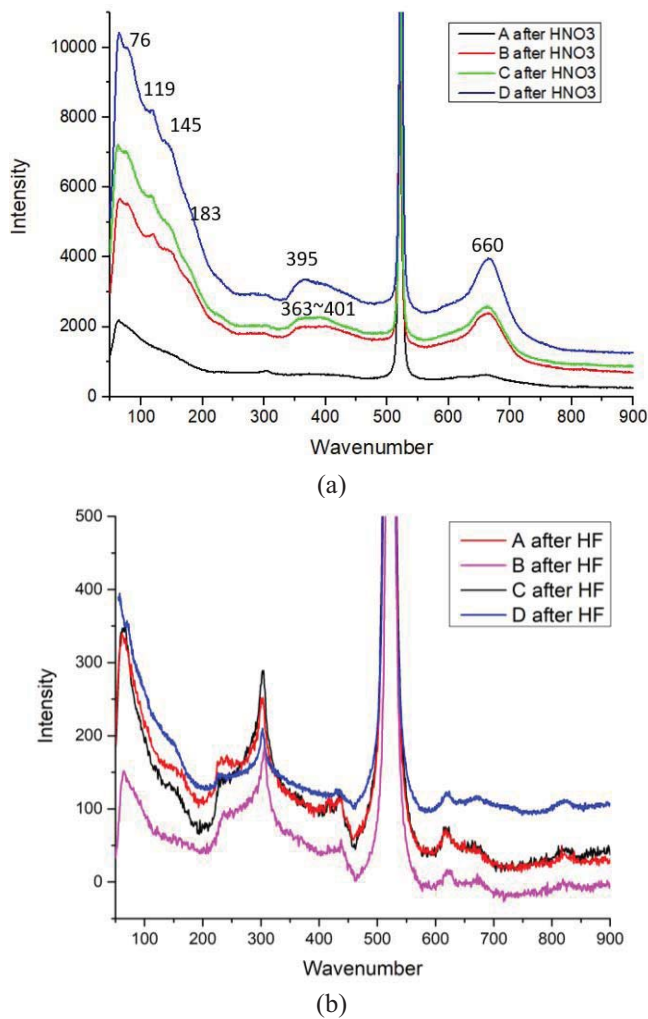
Fig. 1. Raman spectra for the four samples (a) after HNO_3 treatment; (b) after HF treatment

C. SEM and EDX

Fig. 2 shows the SEM under BEC mode for the samples after HNO_3 etched. For paste A, less metal crystallites is observed, while on D, the metal crystallites cover more area and some of them are large. TABEL II shows the EDX analyzes of the element composition in the red box of Fig 2d. The At% of PbM, AgL and TeL are 0.57, 0.30 and 0.26 respectively, which means it is possible that the metal contains both Ag_2Te and PbTe.
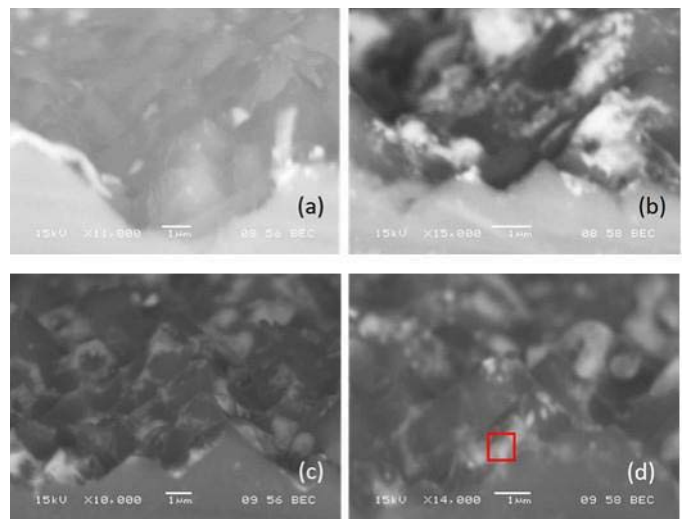
Fig. 2. Back-scattering electron images of (a) sample A; (b) sample B; (c) sample C; (b) sample D after HNO_3 treatment.

After HF etching, the interface glass layer is removed and only the metal crystallites penetrated into the emitter remained in Fig 3. Compared to Fig 2(b), most metal crystallites (Ag_2Te and PdTe) are removed with the glass layer. This indicates that Ag_2Te and PdTe crystallites are encapsulated in the glass layer. For the lowest contact resistivity of paste D, the metal crystallites in the glass layer play a more import role in electron transport than the metal in Si. This corroborates the work of Qi et al on the effect of Pb-Te-O glasses on Ag thick film [15].

TABLE II
EDX ANALYSIS FOR PASTE D

Element	Wt%	At%
CK	23.35	39.83
OK	19.68	25.20
MgK	00.08	00.06
AlK	00.38	00.29
SiK	45.26	33.02
PK	00.00	00.00
PbM	05.74	00.57
BiM	01.78	00.17
ClK	00.20	00.11
AgL	01.57	00.30
CaK	00.33	00.17
TeL	01.65	00.26
Matrix	Correction	ZAF
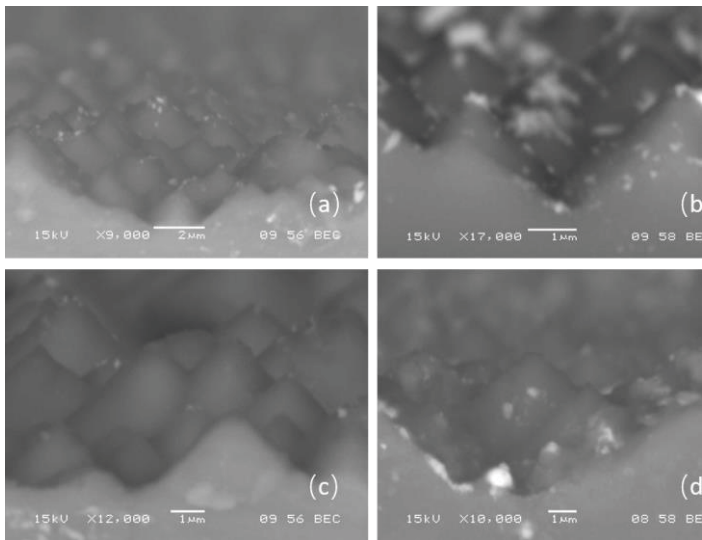
Fig. 3: Back-scattering electron images of (a) sample B; (b) sample C; (c) sample D after HF treatment

V. CONCLUSION

The Raman spectra indicate the formation of Ag_2Te and $PbTe$ in the glass underlying the gridline for pastes B, C, and D. These compounds, These metal crystals play an important role in electron transfer through tunneling. The mechanism of the electron tunneling which bandgap is very small, can heighten the tunneling of electrons from Si into the front Ag gridlines. This could result in the lower contact resistance on the three pastes samples compared to the A counterpart, which did not show these peaks. More so, the SEM reveals that paste A has fewer metal crystallites in the glass layer than paste D. could be resonant tunneling due to the energy bandgap matching between silicon emitter and glass layer. After HF etching, the three peaks observed with HNO_3 treated sample was not observed. From the SEM micrographs after HF dip, less metal crystallites in Si than those embedded in the glass layer after HNO3 treatment. This means that the metal crystallites in the Si are not entirely responsible for current conduction in the front-side contact.

REFERENCES

[1] J. Singh, Semiconductor devices: basic principles: John Wiley & Sons, 2007.

[2] A. Yu, "Electron tunneling and contact resistance of metal-silicon contact barriers," Solid-State Electronics, vol. 13, pp. 239-247, 1970.

[3] E. Cabrera, S. Olibet, J. Glatz-Reichenbach, R. Kopecek, D. Reinke, and G. Schubert, "Current transport in thick film Ag metallization: Direct contacts at Silicon pyramid tips?," Energy Procedia, vol. 8, pp. 540-545, 2011/01/01/ 2011.

[4] S. Kontermann, G. Willeke, and J. Bauer, "Electronic properties of nanoscale silver crystals at the interface of silver thick film contacts on n-type silicon," Applied Physics Letters, vol. 97, p. 191910, 2010.

[5] S. Kontermann, R. Preu, and G. Willeke, "Calculating the specific contact resistance from the nanostructure at the interface of silver thick film contacts on n-type silicon," Applied Physics Letters, vol. 99, p. 111905, 2011.

[6] P. Kumar, M. Pfeffer, B. Willsch, O. Eibl, L. J. Koduvelikulathu, V. D. Mihailetchi, et al., "N-type single-crystalline Si solar cells: Front side metallization for solar cells reaching 20% efficiency," Solar Energy Materials and Solar Cells, vol. 157, pp. 200-208, 2016.

[7] Z. Li, L. Liang, and L. Cheng, "Electron microscopy study of front-side Ag contact in crystalline Si solar cells," ed: AIP, 2009.

[8] R. Hoenig, M. Duerrschnabel, W. van Mierlo, Z. Aabdin, J. Bernhard, J. Biskupek, et al., "The nature of screen printed front side silver contacts-results of the project MikroSol," Energy Procedia, vol. 43, pp. 27-36, 2013.

[9] M. Eberstein, H. Falk-Windisch, M. Peschel, J. Schilm, T. Seuthe, M. Wenzel, et al., "Sintering and Contact Formation of Glass Containing Silver Pastes," Energy Procedia, vol. 27, pp. 522-530, 2012/01/01/ 2012.

[10] M. M. Hilali, S. Sridharan, C. Khadilkar, A. Shaikh, A. Rohatgi, and S. Kim, "Effect of glass frit chemistry on the physical and electrical properties of thick-film Ag contacts for silicon solar cells," Journal of electronic materials, vol. 35, pp. 2041-2047, 2006.

[11] S.-B. Cho, K.-K. Hong, J.-Y. Huh, H. J. Park, and J.-W. Jeong, "Role of the ambient oxygen on the silver thick-film contact formation for crystalline silicon solar cells," Current Applied Physics, vol. 10, pp. S222-S225, 2010/03/01/ 2010.

[12] A. Qin, Y. Fang, P. Tao, J. Zhang, and C. Su, "Silver telluride nanotubes prepared by the hydrothermal method," Inorganic chemistry, vol. 46, pp. 7403-7409, 2007.

[13] T. I. Milenov, T. Tenev, I. Mioushev, G. V. Avdeev, C. W. Luo, and W. C. Chou, "Preliminary studies of the Raman spectra of Ag_2Te and Ag_5Te_3," Optical and Quantum Electronics, journal article vol. 46, no. 4, pp. 573-580, April 01 2014.

[14] B. Zhang, C. Cai, H. Zhu, F. Wu, Y. Ye, Y. Chen, et al., "Phonon blocking by two dimensional electron gas in polar CdTe/PbTe heterojunctions," Applied Physics Letters, vol. 104, p. 161601, 2014.

[15] J. Qin, W. Zhang, S. Bai, and Z. Liu, "Effect of Pb–Te–O glasses on Ag thick-film contact in crystalline silicon solar cells," Solar Energy Materials and Solar Cells, vol. 144, pp. 256-263, 2016.